

DOI: 10.53555/ks.v12i4.3276

Synthesis of Ni doped CNTs Nanocomposites, Their Characterization And Application In The Photodegradation Of Methyl Orange

Sadia Abdul Khaliq¹, Farrukh Bashir^{1*}, Irum Javid², Sumera Shaheen³, Sadaf Saleem³, Zile Huma⁴, Huma Tareen¹, Afroz Rais⁵, Muhammad Aamir Raza⁶

¹Department of Chemistry, Sardar Bahadur Khan Women's University, Quetta-87300, Pakistan

²Department of Biochemistry, Sardar Bahadur Khan Women's University, Quetta-87300, Pakistan

³Department of Biochemistry, Government College Women University, Faisalabad-38000, Pakistan

⁴Department of Zoology, Sardar Bahadur Khan Women's University, Quetta-87300, Pakistan

⁵Department of Botany, Sardar Bahadur Khan Women's University, Quetta-87300, Pakistan

⁶Pakistan Council of Scientific and Industrial Research Laboratories Complex, Quetta-87300, Pakistan

***Corresponding Author:** Dr. Farrukh Bashir

*Email Address: farrukh_chem@yahoo.com

ABSTRACT

Photocatalysis is one of the most sufficient methods used for the removal of organic contaminants from wastewater. In this study, nickel (Ni) doped Carbon nanotubes (CNTs) nanocomposites were tested as a photocatalyst for the methyl orange (MO) dye degradation under irradiation of visible light. Ni doped CNTs nanocomposites were synthesized by using the reduction method. The prepared Ni doped CNTs nanocomposites were characterized using X-ray diffraction (XRD), Fourier-transformed infrared (FTIR) and UV-visible spectroscopy. The degradation of MO dye was carried out by using different amounts (0.05 g, 0.1 g and 5 g) of Ni doped CNTs (with and without acid) at different time intervals. From experiments, it was observed that catalyst Ni doped CNTs without acid showed the highest photocatalytic efficiency for the degradation of MO dye as compared to the catalyst with acid. It was also observed that this efficiency could be enhanced by increasing the amount of the catalyst. Maximum photodegradation (83%) of MO dye was obtained in just 5 minutes when 5 g of the photocatalyst (without acid) was used.

Keywords: Carbon nanotubes, Transition metal, Nanocomposites, Water pollution, Photodegradation

Introduction

Water is used for many different purposes in households, industrial processes, irrigation and electricity production. It gets contaminated when sewage water or wastewater that comes from industrial, commercial and agricultural activities are added to it (Sikdar, 2021). As the human population is increasing the use of water is also increasing (Qadir *et al.*, 2020). It is approximate that the total amount of water on earth is 1.386 billion km³ (333 million cubic miles), with 2.5 % fresh water is available for beneficial use (Fallah-Mehdipour & Haddad, 2015). It is estimated that in Pakistan 32,500 ha area is covered with wastewater and a significant amount of untreated industrial wastewater is dumped into surface bodies (Mahfooz *et al.*, 2020). Wastewater from various origins, such as agriculture, industry and municipal contains different take down of contaminants. These effluents are carcinogenic, non-biodegradable and lethal or toxic in nature (Bhardwaj, Kumar, & Bharadvaja, 2020). In developing countries, one reason for water contamination is due to the discharge of dyes. It is recorded that annually 106 tons of dyes are produced which in turn is a source of water contamination (Pathania *et al.*, 2016). Textile dyes contain more than 50% of azo dyes such as methyl orange (MO), methylene blue (MB) or Congo red. Up to 20% of dyes are lost during dye production in industrial processing and cause environmental pollution (Chowdhury, Hossain, Azad, Islam, & Dewan, 2018). MO which contains nitrogen π -bond, is a more hazardous dye. It serves as a model compound as it is a very ordinary water-resolvable azo dye that is largely used in the pigment of textile fibers, and chemical and paper industries (Behera, Nayak, Banerjee, Chakraborty, & Tripathy, 2021; Radoor, Karayil, Jayakumar, Parameswaranpillai, & Siengchin, 2021). Contamination of MO in water causes toxicity for water bodies like fish, plants as well as humans. It is reported that aromatic amines present in MO are hazardous to human health and cause different diseases like skin or eye irritation, or inhalation of this dye may cause gastrointestinal irritation with vomiting, nausea, and diarrhea (Ismail *et al.*, 2019; Kalra & Gupta, 2021). Bad exposure to MO may increase the heartbeat, jaundice, vomiting, shock, cyanosis, quadriplegia and necrosis (Rezaei Kakhkha, Rezaei Kakhkha, & Faghihi Zarandi, 2017). Researchers are working to develop different methods to remove these contaminants by using different techniques (Raj, Singh, Trivedi, & Soni, 2020). Most of the traditional methods such as adsorption, membrane filtration and chemical treatment are observed to be ineffective for the complete removal of dyes. As these methods merely transfer dye from water to solid and also generate secondary pollutants (such as sludge, toxic gases and solid wastes) and further treatment will be required for the ultimate solution (Balcha, Yadav, & Dey, 2016).

Studies indicated that different nanoparticles (bimetallic and trimetallic) could be used as catalysts for the photodegradation of MO (Adeel, Saeed, Khan, Muneer, & Akram, 2021; Bhatti *et al.*, 2019; Kgtle, Sikhivhilu, Ndlovu, & Moloto, 2021; Rafea,

Nazam, Ramli, Mohamed, & Kasim, 2021a; Zhao et al., 2020). Results obtained from these studies are shown in the following Table 1.

Table 1 Different catalysts, their preparation methods and results

Catalyst	Preparation method	Result	Reference
Cobalt/zinc oxide	Precipitation	100% degradation of MO solution in 130 minutes	(Adeel et al., 2021)
Aluminum/ zinc oxide	Sol-gel method	88.87% degradation in 60 minutes	(Rafaie, Nazam, Ramli, Mohamed, & Kasim, 2021b)
Silver/zinc oxide	Solvothermal method	88% degradation of MO in 2 hours	(Bhatti et al., 2019)
Iron /Copper/ Silver	Sol-gel method	100% degradation of MO in 1 minute	(Kgatle et al., 2021)
Copper iron oxide/carbon nanotubes	Microwave irradiation method	97.16% degradation of MO in 5 minutes	(Zhang et al., 2021)

In present study Ni doped CNTs were used as photocatalyst for the degradation of MO under visible light irradiation. Three different amounts of these catalysts were used for the present study. As pH of catalyst also plays an important role in the degradation process, therefore, these catalysts were prepared separately under vigorous mixing in acidic and aqueous medium and named as Ni doped CNTs with and without acids. Characterization of these samples were done by using XRD, FTIR and UV-Visible spectroscopy.

Materials and Methods

For the preparation of Ni doped CNTs nanoparticles, the name of chemical reagents, their chemical formula, molar mass as well as their suppliers are shown in Table 2.

Table 2 Chemical reagent for the formation of Ni doped CNTs nanocomposites

S. No	Chemical Reagent	Chemical Formula	Molar mass (g/mol)	Supplier
1	Nickel Chloride	NiCl ₂	1.296g/mol	Scharlau
2	Sodium Borohydride	NaBH ₄	0.756 g/mol	DAEJUNG
3	Methyl Orange	C ₁₄ H ₁₄ N ₃ NaO ₃ S	0.0041g/mol	Sigma Aldrich
4	Carbon Nanotubes	CNTs		Sigma Aldrich

For the characterization of synthesized samples different Hi-tech instruments were used. Ultraviolet-visible (UV-visible), model: Shimadzu 17000, spectrophotometer was used to study the process of degradation of MO in the presence of synthesized Ni doped CNTs nanocomposites in the range of 200 nm to 800 nm. Fourier-transform infrared (FTIR), Alpha Bruker portable, spectrophotometer was used to characterize the synthesized nanocomposite in the range of 600 cm⁻¹ to 4000 cm⁻¹. X-ray diffraction (XRD) analysis (model: AXS D2 PHASER Bruker) was used to determine the crystallographic structure of the synthesized sample.

Methodology

Three steps were followed for the preparation of the nanocomposite and degradation of MO dye.

First step

An amount of 1.296 g of NiCl₂ salt was dissolved in 50 mL of distilled water in a beaker and kept on the hotplate with constant stirring. Similarly, 0.756 g of NaBH₄ was prepared in 50 mL of distilled water and added drop wise into NiCl₂ solution with constant stirring for 1 hour at room temperature. The green color of NiCl₂ changes into black color. When precipitates were formed reaction was stopped. These precipitates were washed with 1000 mL of distilled water via centrifugation. After washing, these precipitates were dried in the oven at 80 °C.

Second Step

In this step, Ni doped CNTs nanocomposites were prepared by dispersing equal amounts of the above synthesized Ni nanoparticles with CNTs in 50 mL distilled water on constant stirring for 1 hour at room temperature. Later, this solution was sonicated for the next 40 minutes in an ultrasonicator. In the end, this solution was centrifuged and oven dried at 80 °C. Similarly, for the synthesis of acidic Ni-doped CNTs, an equal amount of Ni and CNTs were dispersed in 15 mL of concentrated acetic acid by keeping the solution on constant stirring for 30 minutes at room temperature. Later, this solution was sonicated for the next 40 minutes in an ultrasonicator. In the end, this solution was centrifuged and oven dried at 80 °C.

Photocatalytic activity

The photocatalytic activities of Ni doped CNTs nanocomposites, as a catalyst, were evaluated by degrading methyl orange (MO) dye, as a pollutant, under UV-Visible irradiation. An amount of (0.05 g, 0.1 g, 5 g) of the catalyst with and without acid was used for the photocatalytic degradation of MO. A solution of MO was prepared by dissolving 0.0041g of MO in 250 mL

of distilled water (5×10^{-6} M). The physical adsorption of MO was recorded at different time intervals by keeping the solution on magnetic stirring at room temperature. The following equation was used to calculate the photocatalytic degradation efficiency and de-colorization of MO.

$$\text{Degradation \%} = \frac{C_o - C_t}{C_o} \times 100 \quad (1)$$

Where C_o is the dye's initial concentration C_t is the final concentration during photo-irradiation.

Results and Discussion

Fourier-transform infrared spectroscopy (FTIR)

Figure 1 shows the FTIR spectrum of synthesized Ni nanoparticles. The region between 460 to 580 cm^{-1} represents the presence of Ni nanoparticles as reported (Budipramana, Ersam, & Kurniawan, 2014).

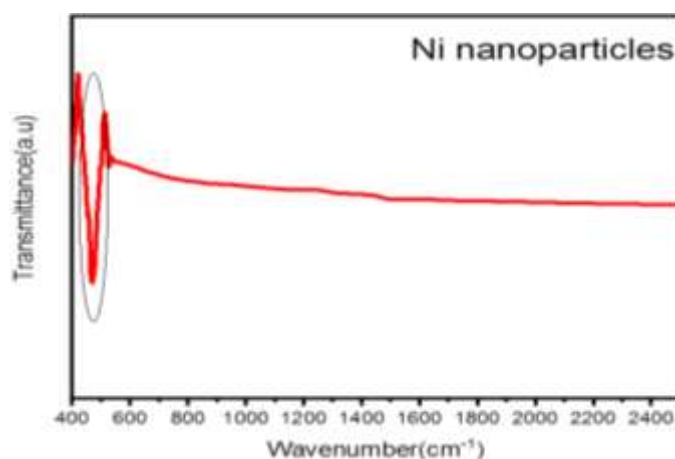


Fig. 1 FTIR spectrum of synthesized Ni nanoparticles

Figure 2 shows the FTIR spectrum of the pure CNTs between the range of 600 to 4000 cm^{-1} . In this spectrum, no specific peak for pure CNTs has been obtained which indicates its purity, as in pure case CNTs have no IR active species. However, the region between 1780 to 2340 cm^{-1} showed the presence of compensated CO_2 in nanotubes. (Lavagna, Massella, & Pavese, 2017).

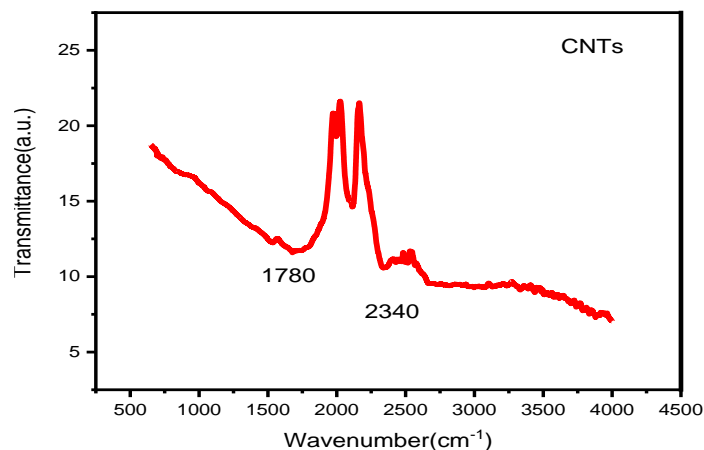


Fig. 2 FTIR spectrum of pure CNTs

Figure 3 shows the FTIR spectrum of synthesized Ni doped CNTs nanocomposites. In the formation of this nanocomposite, the region shows the presence of Ni nanoparticles (which were in the range between 460 to 580 cm^{-1}), has been shifted towards 500-530 cm^{-1} . This shift shows the binding between CNTs and Ni nanoparticles as there are no other components present in them.

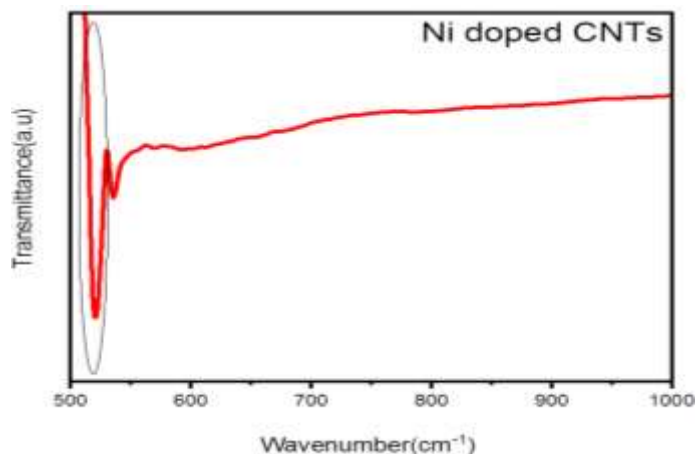


Fig. 3 FTIR spectrum of Ni doped CNTs nanocomposites

X-ray diffraction spectroscopy (XRD)

Sample crystallographic structure was studied by XRD. Figure 4 shows the XRD pattern of nickel nanoparticles with diffraction peaks of 2 theta at 34°, 45° and 60° assigned to (111), (200) and (220) miller indices having face-centered cubic (fcc) Ni structure. These values are well matched with the literature (Barzinjy, Hamad, Aydın, Ahmed, & Hussain, 2020a, 2020b; Hu et al., 2019; Nguyen et al., 2018; Patil, Jadhav, Dubal, & Puri, 2016; Sagadevan & Podder, 2015; Sun, Zhao, Liu, Wang, & Yan, 2017).

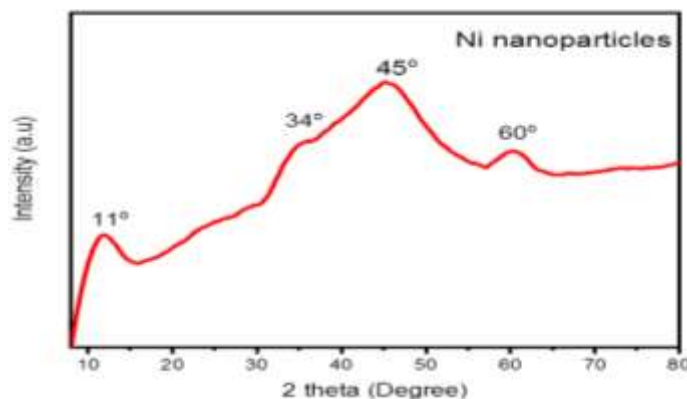


Fig. 4 XRD pattern of Ni nanoparticles

Figure 5 shows the XRD structure of pure CNTs with sharp diffraction peaks at 25°, 42° assigned to (111) and (100) are well matched with previously reported work (Abdulrazzak, Alkiam, & Hussein, 2019; Ali, Shah, Ahmad, Nawab, & Huang, 2019; Fathi, Nejad, Mahmoodzadeh, & Satari, 2017; Saravanan, Prasad, Gokulakrishnan, Kalaivani, & Somanathan, 2014; Soleimani et al., 2015; Thirumal, Pandurangan, Jayavel, Krishnamoorthi, & Ilangovan, 2016).

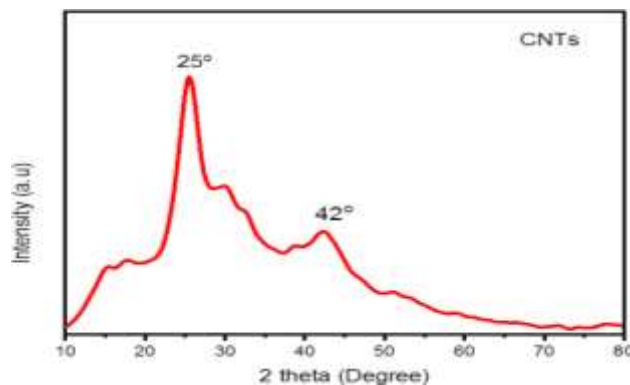


Fig. 5 XRD pattern of pure CNTs

Figure 6 indicates the XRD pattern of Ni doped CNTs (without acid) nanocomposite. The characteristic peaks of 2 theta at 60° assigned to (220) correspond the crystallographic orientations for Ni nanoparticles (Fazlali, reza Mahjoub, & Abazari, 2015; Parsaee, 2018; Sabouri et al., 2020). The diffraction peak of 2 theta at 26° is assigned to (002) which indicates the CNTs crystallographic structure (Li et al., 2015; Nie et al., 2015; Selen, Güler, Özer, & Evin, 2016). Ni and CNTs reduce their characteristic peaks at 45° and 42° with a new peak at 36° indicating their successful combination in the form of a composite. Similarly, Figure 7 shows the XRD pattern of Ni doped CNTs (with acid) nanocomposite. The characterized peaks of the nanocomposite of Ni doped CNTs (with acid) are also shifted from 45° to 47° and 60° to 64°, respectively.

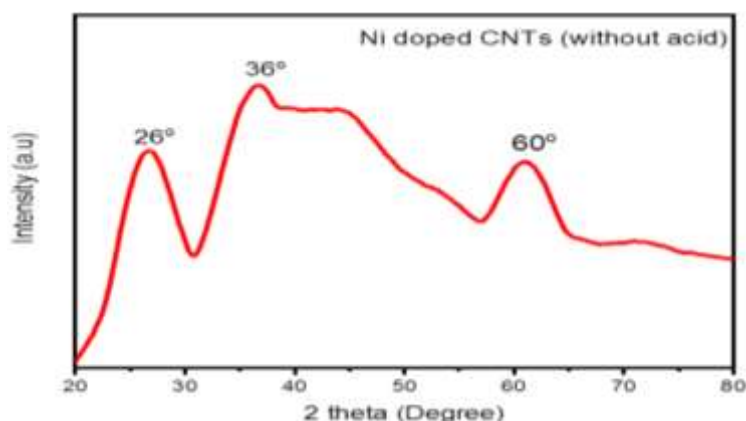


Fig. 6 XRD pattern of Ni doped CNTs (without acid) nanocomposites

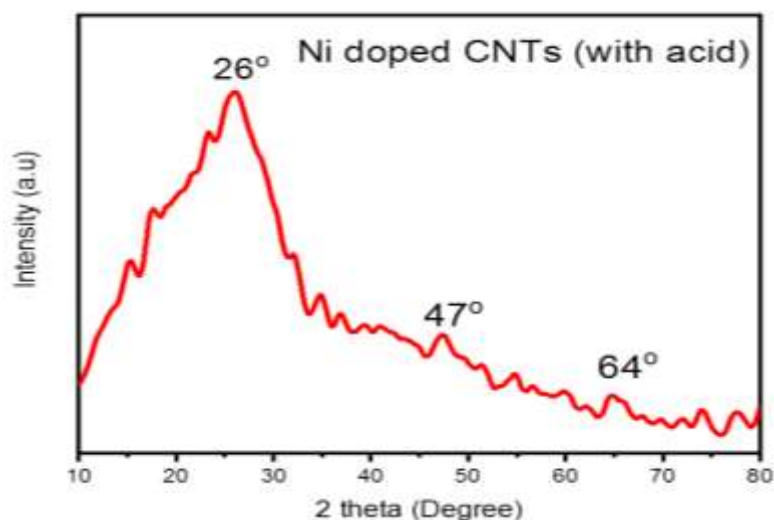


Fig. 7 XRD pattern of Ni doped CNTs (with acid) nanocomposites

Photocatalytic Activity

The photocatalytic activity of the nanocomposites of Ni doped CNTs (with and without acid) was carried out for MO dye degradation at different time intervals by using UV-visible spectroscopy.

Degradation of MO dye by using Ni doped CNTs (without acid)

The photocatalytic degradation of MO dye was studied by using 0.05 g, 0.1 g, and 5 g nanocomposites of Ni doped CNTs without acid. From the results, it was observed that by using a 0.05 g catalyst the degradation of MO dye was 84 % in 120 minutes, the catalyst with 0.1 g amount degraded 75 % of the MO dye in 15 minutes and on the other hand by using 5 g catalyst the degradation rate was reached to 83 % in just 5 minutes. Figure 8 depicted that the degradation rate of MO solution was increased by increasing the amount of Ni doped CNTs (without acid). Figure 9 and Figure 10 show the discoloration and removal efficiency of MO by using the catalyst (without acid).

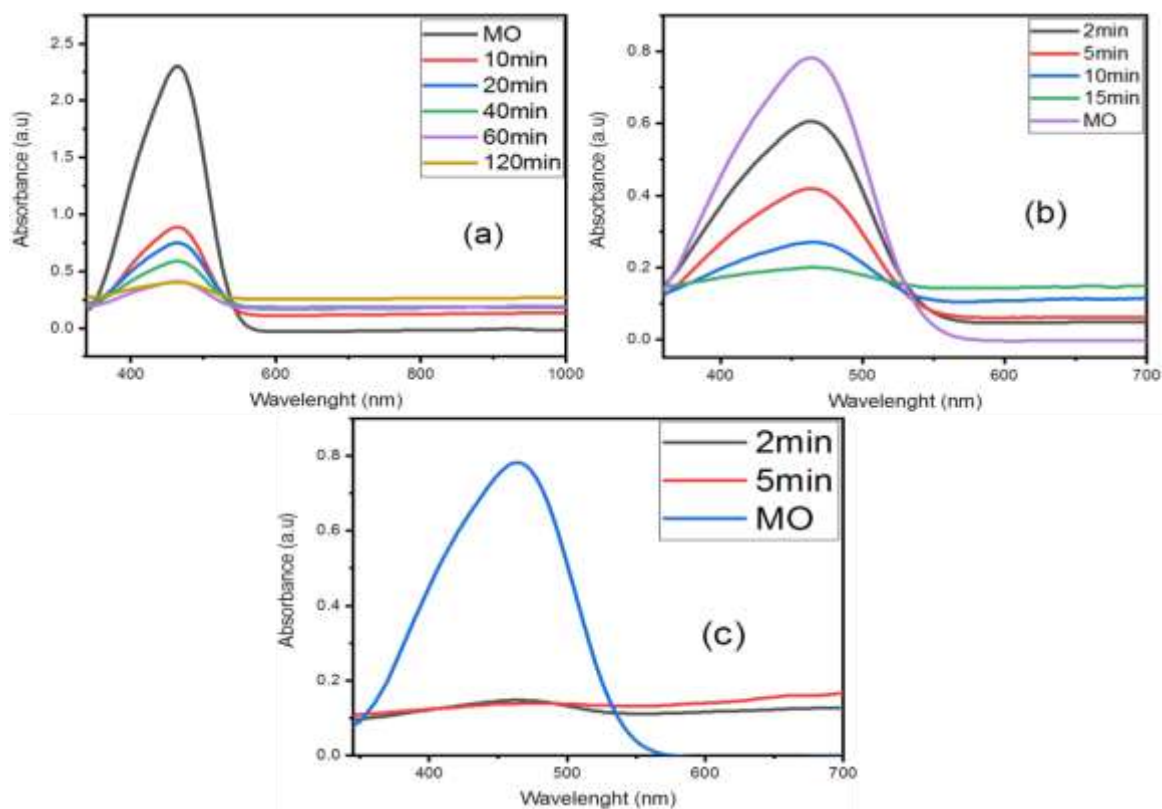


Fig. 8 Photocatalytic degradation of MO dye by using nanocomposites of (a) 0.05 g, (b) 0.1 g, (c) 5 g Ni doped CNTs (without acid)



Fig. 9 Photocatalytic degradation of MO solution by using (a) 0.05 g, (b) 0.1 g, (c) 5 g of Ni doped CNTs (without acid)

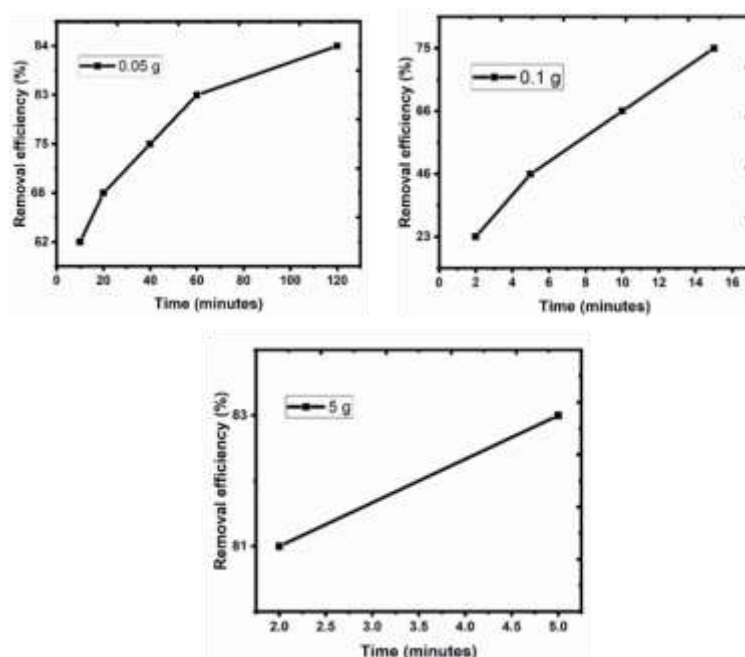


Fig. 10 Percentage degradation of MO dye by using different nanocomposites of Ni doped CNTs (without acid)

Degradation of MO dye using nanocomposites of Ni doped CNTs (with acid)

The photocatalytic activity of MO dye was studied by using 0.05 g, 0.1 g, and 5 g of Ni doped CNTs (with acid). MO shows a yellow color in the blue spectrum region at about (430 – 480 nm). With the addition of acid, the spectrum was changed from the blue spectrum region to the cyan region (500 - 520 nm) (Shamsipur, Barati, & Karami, 2017). In the present study, the λ_{max} of MO was obtained at 464 nm. However, by the addition of the catalyst (with acid), it was shifted towards the cyan region with λ_{max} at about 520 nm. As reported the change in the region is due to the addition of hydrogen ion which causes the breakage of the nitrogen-nitrogen double bond and takes its one nitrogen that causes the delocalization of a positive charge on nitrogen. This increase in delocalization also increases the wavelength (Clark, 2017). Therefore, the addition of an acidic catalyst in the present study increased the delocalization in MO as the reaction proceeded at different time intervals. The photocatalytic analysis (as shown in Figure 11) of MO showed that with 0.05 g of catalyst, about 45 % of MO solution was degraded in 60 minutes, while with 0.1g of catalyst, the degradation was just 11% in 120 minutes, however, with the use of 5g of catalyst the degradation rate was increased up to 69 % in just 9 minutes. Figure 12, shows the discoloration of the dye at different time intervals with different contents of the nanocomposites. Figure 13 shows the %removal efficiency of the MO degradation with respect to time.

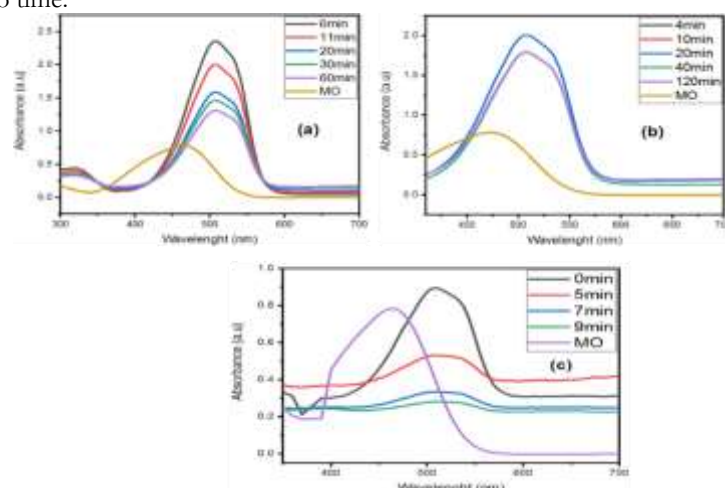


Fig. 11 Photocatalytic degradation of MO dye by using nanocomposites of (a) 0.05 g, (b) 0.1 g and (c) 5 g Ni doped CNTs (with acid)

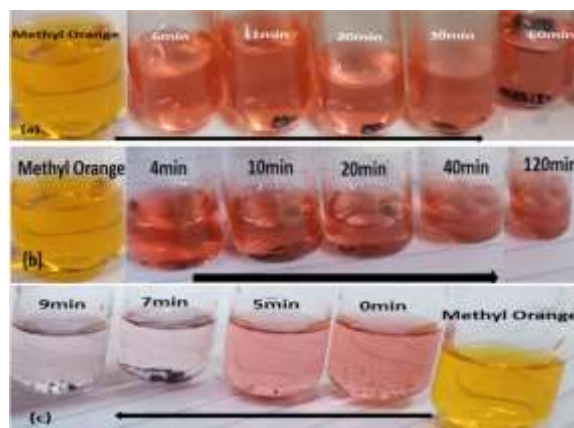


Fig. 12 Photocatalytic degradation of MO solution with different amounts (a) 0.05 g (b) 0.1 g and (c) 5 g nanocomposites of Ni doped CNTs (with acid)

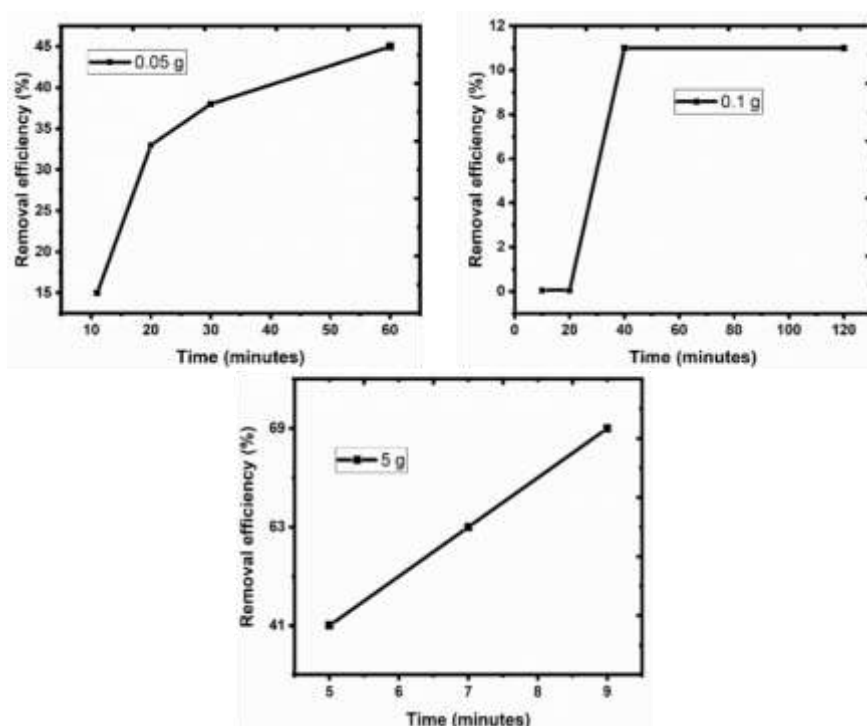
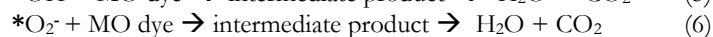
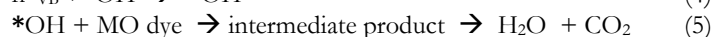
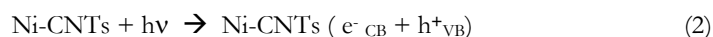


Fig. 13 Percentage degradation of MO dye by using different nanocomposites of Ni doped CNTs (with acid)

From the results, it is predictable from the reported studies that hydroxyl radical ($\cdot\text{OH}$), superoxide radical ($\cdot\text{O}_2^-$) and positive holes (h^+) played vital roles in the photocatalytic processes. The photocatalytic process is a form of heterogeneous reaction where oxidation and reduction take place through redox reactions. Furthermore, it is expected that when the energy levels exceed the band gap, the electrons (e^-) move towards the conduction band while positive holes (h^+) remain in the uppermost valence band region. When holes move toward the surface of CNTs, the space charge layer tries to keep the holes and photogenerated electrons far apart (Dana & Sheibani, 2021). When Ni doped CNTs interact with photons, they react either with adsorbed water or OH^- ions available on the surface and generate the $\cdot\text{OH}$ radicals by the initiation of a vigorous oxidation reaction (Lassoued, Lassoued, Dkhil, Ammar, & Gadri, 2018).



It was observed that with increasing the amount of Ni doped CNTs nanocomposites the photocatalytic degradation efficiency was also increased. Photocatalytic degradation results depicted that as the quantity of the catalyst (both with and without acid) was increased, the time for the degradation of dye was reduced. Adhikari and his friend (Adhikari & Madras, 2017) synthesized NiO/Ni catalyst and found that the catalyst combusted in citric acid degraded only 48% of rhodamine 6G (RG) in 3 hours. Dana and his friend fabricated CNTs/CuO nanocomposites via copper electroless deposition on CNTs at different time durations (30, 60 and 120 minutes). They analyzed the photocatalytic degradation of methylene blue (MB) and MO by using

these catalysts and found that the degradation efficiency was significantly higher for MB than for MO (Dana & Sheibani, 2021). In the present study, results obtained by using Ni doped CNTs without acid showed that the % removal efficiency of the catalyst at the lowest concentration was almost the same as that of at higher concentration. It may be attributed that the dispersion of the catalyst at lower concentration was maximum and the availability of the pores on CNTs surfaces was maximum (Mohamed, Ghazali, Kassem, Elgazzar, & Mostafa, 2022) which resulted in the increased degradation rate but the equilibrium was established slowly as the concentration was low. However, at higher catalytic concentration, the availability of active sites of the transition metals along with the pores of CNTs was significantly maximum, therefore, less time was taken to approach the equilibrium with a higher % removal efficiency. Another important factor to be observed by the results suggested that the % removal efficiency of the catalysts with acid was comparatively less. The synthesis of Ni doped CNTs in acetic acid may introduce the carboxylic group from acid into the graphene structure (pores) of CNTs which may reduce the π - π interactions between the rings of MO and Ni and result in the decrease in the % removal efficiency of the catalyst. Overall, CNTs enhance the photocatalytic activity of the catalyst by providing a platform for the transfer of electrons between Ni and molecules of MO via π - π interactions between the aromatic rings of MO and CNTs.

Conclusion

Different content-based Ni doped CNTs (with and without acid) were synthesized by using a simple mixing method. Characterization done by XRG and FTIR justifies the successful formation of these nanocomposites. When these nanocomposites were used as catalysts for the photodegradation of MO, it was observed that with increasing the amount of Ni doped CNTs, the photocatalytic degradation efficiency was also increased and maximum photodegradation of MO dye was obtained when 5g without acid catalyst was used and degradation rate was reached up to 83% in just 5 minutes. However, other quantities of the catalysts (with and without acid) also showed better degradation rates. Overall, the present study justifies that the nanocomposites of Ni doped CNTs are good catalysts for the degradation of MO dyes from wastewater.

CRedit Author Statement

Conceptualization, literature survey, methodology, analysis and results interpretation were done by **Sadia Abdul Hayee, Dr. Farrukh Bashir and Muhammad Aamir Raza** whereas drafting, editing, reviewing and result discussion were done by **Dr. Irum Javid, Dr. Sumera Shaheen, Dr. Sadaf Saleem, Dr. Zile Huma, Huma Tareen and Dr. Afroz Rais**.

Conflict of interest

The authors affirm the absence of any conflicting interests.

References:

1. Abdulrazzak, F. H., Alkiam, A. F., & Hussein, F. H. (2019). Behavior of X-ray analysis of carbon nanotubes. In *Perspective of Carbon Nanotubes*: IntechOpen.
2. Adeel, M., Saeed, M., Khan, I., Muneer, M., & Akram, N. (2021). Synthesis and characterization of Co-ZnO and evaluation of its photocatalytic activity for photodegradation of methyl orange. *ACS omega*, 6(2), 1426-1435.
3. Adhikari, S., & Madras, G. (2017). Role of Ni in hetero-architected NiO/Ni composites for enhanced catalytic performance. *Physical Chemistry Chemical Physics*, 19(21), 13895-13908.
4. Ali, S., Shah, I. A., Ahmad, A., Nawab, J., & Huang, H. (2019). Ar/O₂ plasma treatment of carbon nanotube membranes for enhanced removal of zinc from water and wastewater: a dynamic sorption-filtration process. *Science of the total environment*, 655, 1270-1278.
5. Balcha, A., Yadav, O. P., & Dey, T. (2016). Photocatalytic degradation of methylene blue dye by zinc oxide nanoparticles obtained from precipitation and sol-gel methods. *Environmental Science and Pollution Research*, 23(24), 25485-25493.
6. Barzinjy, A. A., Hamad, S. M., Aydın, S., Ahmed, M. H., & Hussain, F. H. (2020a). Green and eco-friendly synthesis of Nickel oxide nanoparticles and its photocatalytic activity for methyl orange degradation. *Journal of Materials Science: Materials in Electronics*, 31(14), 11303-11316.
7. Barzinjy, A. A., Hamad, S. M., Aydın, S., Ahmed, M. H., & Hussain, F. H. (2020b). Green and eco-friendly synthesis of Nickel oxide nanoparticles and its photocatalytic activity for methyl orange degradation. *Journal of Materials Science: Materials in Electronics*, 31, 11303-11316.
8. Behera, M., Nayak, J., Banerjee, S., Chakraborty, S., & Tripathy, S. K. (2021). A review on the treatment of textile industry waste effluents towards the development of efficient mitigation strategy: An integrated system design approach. *Journal of Environmental Chemical Engineering*, 105277.
9. Bhardwaj, D., Kumar, L., & Bharadvaja, N. (2020). A review on sources of dyes, sustainable aspects, environmental issues and degradation methods. *India 2020: Environmental Challenges, Policies and Green Technology*, 137.
10. Bhatti, M. A., Shah, A. A., Almani, K. F., Tahira, A., Chalanger, S. E., dad Chandio, A., . . . Ibupoto, Z. H. (2019). Efficient photo catalysts based on silver doped ZnO nanorods for the photo degradation of methyl orange. *Ceramics International*, 45(17), 23289-23297.
11. Budipramana, Y., Ersam, T., & Kurniawan, F. (2014). Synthesis nickel hydroxide by electrolysis at high voltage. *Journal of Engineering & Applied Sciences*.
12. Chowdhury, M., Hossain, M., Azad, M., Islam, M., & Dewan, M. (2018). Photocatalytic degradation of methyl orange under UV using ZnO as catalyst. *Int. J. Sci. Eng. Res*, 9(6).
13. Clark, J. (2017). What causes molecules to absorb UV and visible light. Retrieved July, 31, 2017.
14. Dana, A., & Sheibani, S. (2021). CNTs-copper oxide nanocomposite photocatalyst with high visible light degradation efficiency. *Advanced Powder Technology*, 32(10), 3760-3769.

15. Fallah-Mehdipour, E., & Haddad, O. B. (2015). Application of genetic programming in hydrology. In *Handbook of Genetic Programming Applications* (pp. 59-70): Springer.
16. Fathi, Z., Nejad, R.-A. K., Mahmoodzadeh, H., & Satari, T. N. (2017). Investigating of a wide range of concentrations of multi-walled carbon nanotubes on germination and growth of castor seeds (*Ricinus communis* L.). *Journal of plant protection research*.
17. Fazlali, F., reza Mahjoub, A., & Abazari, R. (2015). A new route for synthesis of spherical NiO nanoparticles via emulsion nano-reactors with enhanced photocatalytic activity. *Solid State Sciences*, 48, 263-269.
18. Hu, Q., Li, W., Abouelamaiem, D. I., Xu, C., Jiang, H., Han, W., & He, G. (2019). Hollow Cu-doped NiO microspheres as anode materials with enhanced lithium storage performance. *RSC advances*, 9(36), 20963-20967.
19. Ismail, M., Akhtar, K., Khan, M., Kamal, T., Khan, M. A., M Asiri, A., . . . Khan, S. B. (2019). Pollution, toxicity and carcinogenicity of organic dyes and their catalytic bio-remediation. *Current pharmaceutical design*, 25(34), 3645-3663.
20. Kalra, A., & Gupta, A. (2021). Recent advances in decolourization of dyes using iron nanoparticles: A mini review. *Materials Today: Proceedings*, 36, 689-696.
21. Kgatle, M., Sikhwivhilu, K., Ndlovu, G., & Moloto, N. (2021). Degradation kinetics of methyl orange dye in water using trimetallic Fe/Cu/Ag nanoparticles. *Catalysts*, 11(4), 428.
22. Lassoued, A., Lassoued, M. S., Dkhil, B., Ammar, S., & Gadri, A. (2018). RETRACTED ARTICLE: Photocatalytic degradation of methyl orange dye by NiFe 2 O 4 nanoparticles under visible irradiation: Effect of varying the synthesis temperature. *Journal of Materials Science: Materials in Electronics*, 29, 7057-7067.
23. Lavagna, L., Massella, D., & Pavese, M. (2017). Preparation of hierarchical material by chemical grafting of carbon nanotubes onto carbon fibers. *Diamond and Related Materials*, 80, 118-124.
24. Li, J., Ye, S., Li, T., Li, X., Yang, X., & Ding, S. (2015). Preparation of graphene nanoribbons (GNRs) as an electronic component with the multi-walled carbon nanotubes (MWCNTs). *Procedia engineering*, 102, 492-498.
25. Mahfooz, Y., Yasar, A., Gujian, L., Islam, Q. U., Akhtar, A. B. T., Rasheed, R., . . . Naeem, U. (2020). Critical risk analysis of metals toxicity in wastewater irrigated soil and crops: a study of a semi-arid developing region. *Scientific reports*, 10(1), 1-10.
26. Mohamed, R. A., Ghazali, N. M., Kassem, L. M., Elgazzar, E., & Mostafa, W. A. (2022). Synthesis of MnCoO/CNT nanoflakes for the photocatalytic degradation of methyl orange dye and the evaluation of their activity against *Culex pipiens* larvae in the purification of fresh water. *RSC Adv*, 12(45), 29048-29062. doi:10.1039/d2ra04823j
27. Nguyen, K., Hoa, N. D., Hung, C. M., Le, D. T. T., Van Duy, N., & Van Hieu, N. (2018). A comparative study on the electrochemical properties of nanoporous nickel oxide nanowires and nanosheets prepared by a hydrothermal method. *RSC advances*, 8(35), 19449-19455.
28. Nie, P., Min, C., Song, H.-J., Chen, X., Zhang, Z., & Zhao, K. (2015). Preparation and tribological properties of polyimide/carboxyl-functionalized multi-walled carbon nanotube nanocomposite films under seawater lubrication. *Tribology Letters*, 58, 1-12.
29. Parsaei, Z. (2018). Synthesis of novel amperometric urea-sensor using hybrid synthesized NiO-NPs/GO modified GCE in aqueous solution of cetrimonium bromide. *Ultrasonics sonochemistry*, 44, 120-128.
30. Pathania, D., Gupta, D., Ala'a, H., Sharma, G., Kumar, A., Naushad, M., . . . Alshehri, S. M. (2016). Photocatalytic degradation of highly toxic dyes using chitosan-g-poly (acrylamide)/ZnS in presence of solar irradiation. *Journal of Photochemistry and Photobiology A: Chemistry*, 329, 61-68.
31. Patil, S., Jadhav, L., Dubal, D., & Puri, V. (2016). Characterization of NiO-Al₂O₃ composite and its conductivity in biogas for solid oxide fuel cell.
32. Qadir, M., Drechsel, P., Jiménez Cisneros, B., Kim, Y., Pramanik, A., Mehta, P., & Olaniyan, O. (2020). *Global and regional potential of wastewater as a water, nutrient and energy source*. Paper presented at the Natural Resources Forum.
33. Radoor, S., Karayil, J., Jayakumar, A., Parameswaranpillai, J., & Siengchin, S. (2021). Efficient removal of methyl orange from aqueous solution using mesoporous ZSM-5 zeolite: Synthesis, kinetics and isotherm studies. *Colloids and Surfaces A: Physicochemical and Engineering Aspects*, 611, 125852.
34. Rafaie, H. A., Nazam, N. A. A. M., Ramli, N. I. T., Mohamed, R., & Kasim, M. F. (2021a). Synthesis, characterization and photocatalytic activities of Al-doped ZnO for degradation of methyl orange dye under UV light irradiation. *Journal of the Australian Ceramic Society*, 57, 479-488.
35. Rafaie, H. A., Nazam, N. A. A. M., Ramli, N. I. T., Mohamed, R., & Kasim, M. F. (2021b). Synthesis, characterization and photocatalytic activities of Al-doped ZnO for degradation of methyl orange dye under UV light irradiation. *Journal of the Australian Ceramic Society*, 57(2), 479-488.
36. Raj, S., Singh, H., Trivedi, R., & Soni, V. (2020). Biogenic synthesis of AgNPs employing *Terminalia arjuna* leaf extract and its efficacy towards catalytic degradation of organic dyes. *Scientific reports*, 10(1), 1-10.
37. Rezaei Kakhkha, M. R., Rezaei Kakhkha, B., & Faghihi Zarandi, A. (2017). Sonocatalysis degradation of methyl orange using zinc sulfide carbon nanotubes nanocatalyst. *Advances in Environmental Technology*, 3(4), 243-248.
38. Sabouri, Z., Fereydouni, N., Akbari, A., Hosseini, H. A., Hashemzadeh, A., Amiri, M. S., . . . Darroudi, M. (2020). Plant-based synthesis of NiO nanoparticles using *salvia macrosiphon* Boiss extract and examination of their water treatment. *Rare Metals*, 39(10), 1134-1144.
39. Sagadevan, S., & Podder, J. (2015). Investigations on structural, optical, morphological and electrical properties of nickel oxide nanoparticles. *International Journal of Nanoparticles*, 8(3-4), 289-301.
40. Saravanan, A., Prasad, K., Gokulakrishnan, N., Kalaivani, R., & Somanathan, T. (2014). Efficiency of transition metals in combustion catalyst for high yield helical multi-walled carbon nanotubes. *Advanced Science, Engineering and Medicine*, 6(7), 809-813.

41. Selen, V., Güler, Ö., Özer, D., & Evin, E. (2016). Synthesized multi-walled carbon nanotubes as a potential adsorbent for the removal of methylene blue dye: kinetics, isotherms, and thermodynamics. *Desalination and water treatment*, 57(19), 8826-8838.
42. Shamsipur, M., Barati, A., & Karami, S. (2017). Long-wavelength, multicolor, and white-light emitting carbon-based dots: Achievements made, challenges remaining, and applications. *Carbon*, 124, 429-472.
43. Sikdar, P. K. (2021). Environmental Management: Issues and Concerns. *Environmental Management: Issues and Concerns in Developing Countries*, 1-21.
44. Soleimani, H., Yahya, N., Baig, M., Khodapanah, L., Sabet, M., Burda, M., . . . Awang, M. (2015). Synthesis of carbon nanotubes for oil-water interfacial tension reduction. *Oil Gas Res*, 1(1), 1000104.
45. Sun, D.-L., Zhao, B.-W., Liu, J.-B., Wang, H., & Yan, H. (2017). Application of nickel oxide nanoparticles in electrochromic materials. *Ionics*, 23, 1509-1515.
46. Thirumal, V., Pandurangan, A., Jayavel, R., Krishnamoorthi, S., & Ilangoan, R. (2016). Synthesis of nitrogen doped coiled double walled carbon nanotubes by chemical vapor deposition method for supercapacitor applications. *Current Applied Physics*, 16(8), 816-825.
47. Zhang, W., Liang, Q., Huang, J., Shao, B., Liu, Y., Liu, Y., . . . Yan, M. (2021). Microwave-Assisted High-Efficiency Degradation of Methyl Orange by using CuFe₂O₄/CNTs Catalysts and Insight into Degradation Mechanism.
48. Zhao, C., Guo, J., Yu, C., Zhang, Z., Sun, Z., & Piao, X. (2020). Fabrication of CNTs-Ag-TiO₂ ternary structure for enhancing visible light photocatalytic degradation of organic dye pollutant. *Materials Chemistry and Physics*, 248, 122873.